Supplemental Materials and Methods

Yeast media and cell growth

Yeast were grown overnight in YPDextrose (YPD) or YPGalactose (YPG), then diluted and grown to mid-logarithmic growth phase. For pronging, cells were serially diluted 1:1 with sterile water into 96-well plates. A steel prong was used to stamp plates with or without drugs as indicated in the figure legends. For viability plating, cells were diluted in sterile water and spread with sterile glass beads on plates with or without drugs. After incubation, single colonies were counted. Percent viability is calculated relative to colony number on YPG. All plates were incubated at 24°C. Growth rates were determined by diluting overnight cultures to an OD_{660} of 0.15. Cultures were incubated at 24°C for a total of 8 hours. OD_{660} was measured every hour. To determine bud size for cell cycle progression analysis, population images of log phase cultures were acquired at 24°C and categorized by eye. Strains are indicated in "SI Appendix, Table S4".

Plates and Media

YPD and YPG+5 mM or 10mM HU plates were made from 1 M HU stock in water. YPD and YPG +0.2 µg/mL PHL plates were made from 0.1 mg/mL PHL stock in water. YPD+100 or 200 µg/mL etoposide plates were made from a 50 mg/mL etoposide stock in DMSO. YPD+0.5 µg/mL and 2.5 µg/mL benomyl plates were made from a 50 µg/mL benomyl stock in DMSO.

Phleomycin is a glycopeptide antibiotic of the bleomycin family, that is widely used as an agent to induce DSB (1). HU is an inhibitor of ribonucleotide reductase (2).

PCR analysis of rearranged centromeres

Primers for GALCEN3-CEN3 recombination were 3050 (TCGACTACGCGATCATGGCG) and 3320 (GGGTGGGAAACTGAAGAAATC)("SI Appendix, Figure S4"); GALCEN3 deletion 3050 and 3051 (cacgatgcgtccggcgtaga) (Fig. 2); CEN3 deletion 2837 (ggatcagcgccaaacaatatgg) and 3320 (Fig. 2). Quantitative PCR for rearrangements in PHL were performed with oligonucleotides 3050 and 3320. Template dilutions are indicated in the graphical representation ("SI Appendix, Figure S4").

Simulation

ChromoShake is a thermodynamics simulator initially constructed to determine the thermodynamically favored states of chromosomal elements (3). The model uses a series of beads, associated to one another with springs and hinges, and simulates the movement of the beads by Brownian motion. Each bead in the simulation represents 10 nm or about 30 bp of b-form DNA. We introduced a 1-micron chain of double-stranded DNA, modeled using a bead-spring construct, with a replication bubble of 350 nm in the center of the chain. In both iterations of the simulation, the beads on the two ends of this chain began two orders of magnitude more massive than the rest of the simulation beads to resist pulling and mimic the force produced by DNA polymerase in replication. The centromeres were labeled in green at the origin of replication on the two daughter strands.

Both versions of the simulation were initially iterated in ChromoShake for a period of time (700 microseconds). In the 'pinned' simulation, which represents continuous action of DNA polymerase, the end beads remained two orders of magnitude larger throughout the total simulation time in

ChromoShake (18.2 milliseconds). In the 'unpinned' simulation, which represents a pause in replication and the removal of the force generated by DNA polymerase, the mass of the two end beads was reduced to that of a standard bead and the simulation was iterated in ChromoShake for the same period of time as the 'pinned' simulation.

Each simulation was run a total of three times, with different random seeds. In each simulation, the ratio of the distance between the two centromere beads to the distance between the two beads at the replication fork was calculated at all time points for each simulation. This ratio was used to determine the aspect ratio of the replication bubble over time and was compared between the two versions of the simulation.

3C Protocol

Cells were grown overnight in rich media. Dicentric *chl4Δ* was grown in YPD, WT dicentric was grown in YPG. Cells were then diluted and grown for 3 hours under various conditions. For the drug treatments, PHL was added to 0.2µg/mL and HU was added to 10mM. For the WT dicentric glu treatment, cells were switched from YPG to YPD.

Yeast nuclei were prepared and crosslinked with 1% formaldehyde for 10 min at room temperature, with the goal of crosslinking any regions of the genome that were in physical proximity to one another. The reaction was quenched with the addition of glycine to 0.25M. Nuclei were washed and resuspended in appropriate 1X restriction digest buffer. 1% SDS was added, and the nuclei were incubated at 65°C for 10 min to remove uncrosslinked proteins. Triton X-100 was added to a final concentration of 1% to remove the SDS and allow for subsequent digestion. 150 units of the restriction enzyme NsiI (Mph1103I) were added, and the reaction was incubated overnight at 37°C. 60 units of NsiI were added and the reaction was incubated for an additional hour at 37 °C. 10% SDS was added to each tube and incubated at 65°C for 20 min to inactivate NsiI. 800 cohesive end units of T4 DNA ligase were added, and the reaction was incubated at 16°C for 6 hours to ligate crosslinked DNA. Crosslinks were then reversed with the addition of proteinase K and overnight incubation at 65°C. DNA was purified by phenol-chloroform extraction and ethanol precipitation. DNA concentration was determined by running 1% agarose gels and staining with ethidium bromide. All gels were imaged with an Alpha Innotech AlphaImager 2200 imaging system, and all images were imported into Metamorph 7.7 for analysis. Gels were analyzed by measurement of the integrated intensity of a band and correcting for background as described in Hoffman et al., (4). Computer-generated boxes 5 x 5 and 6 x 6 pixel regions were centered over each band, and the total integrated fluorescence counts were obtained for each region. The measured value for the 5 x 5 pixel region includes both product fluorescence and local background fluorescence. The background component was obtained by subtraction of the integrated value of the 5 x 5 pixel region from the larger 6 x 6 pixel region. This result was scaled in proportion to the smaller area of the 5 x 5 pixel region and then subtracted from the integrated value of the 5 x 5 pixel region to yield a value for product fluorescence. This method controls for inhomogeneity in background fluorescence.

The crosslinking frequency of two regions of chromosome III were compared. One region, 3584 base pairs in length, spanned GALCEN at HIS4, bordered on either side by NsiI cut sites, one site being 68903 (chrIII coordinate), 1700 base pairs upstream of GALCEN3 and the other being 65319 (chrIII coordinate), 1900 base pairs downstream of GALCEN3. The other region, 7065 base pairs in length, was located approximately 165 kb from GALCEN3, with one NsiI cut site 233048 bp and the other 225983 bp. Ligation products from these regions were detected by PCR, yielding products approximately 600-700

base pairs in size. PCR products from crosslinked DNA were compared to identical products generated from control DNA (naked DNA) that was not crosslinked.

Supplemental Figures

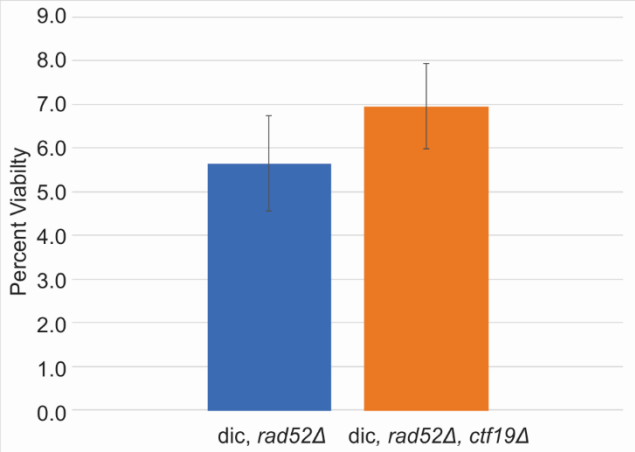

Fig. S1 Quantitative analysis of cell viability in dicentric *rad52Δ* and dicentric *rad52Δ ctf19Δ.* Quantitative analysis of cell viability expressed as a percent of single colony growth on galactose (inactive GALCEN). Deletion of Ctf19 does not suppress breakage of the dicentric chromosome. Error bars are standard error of the mean. Student's T-test p-value 0.457. Dilution plating ns can be found in Table S2.

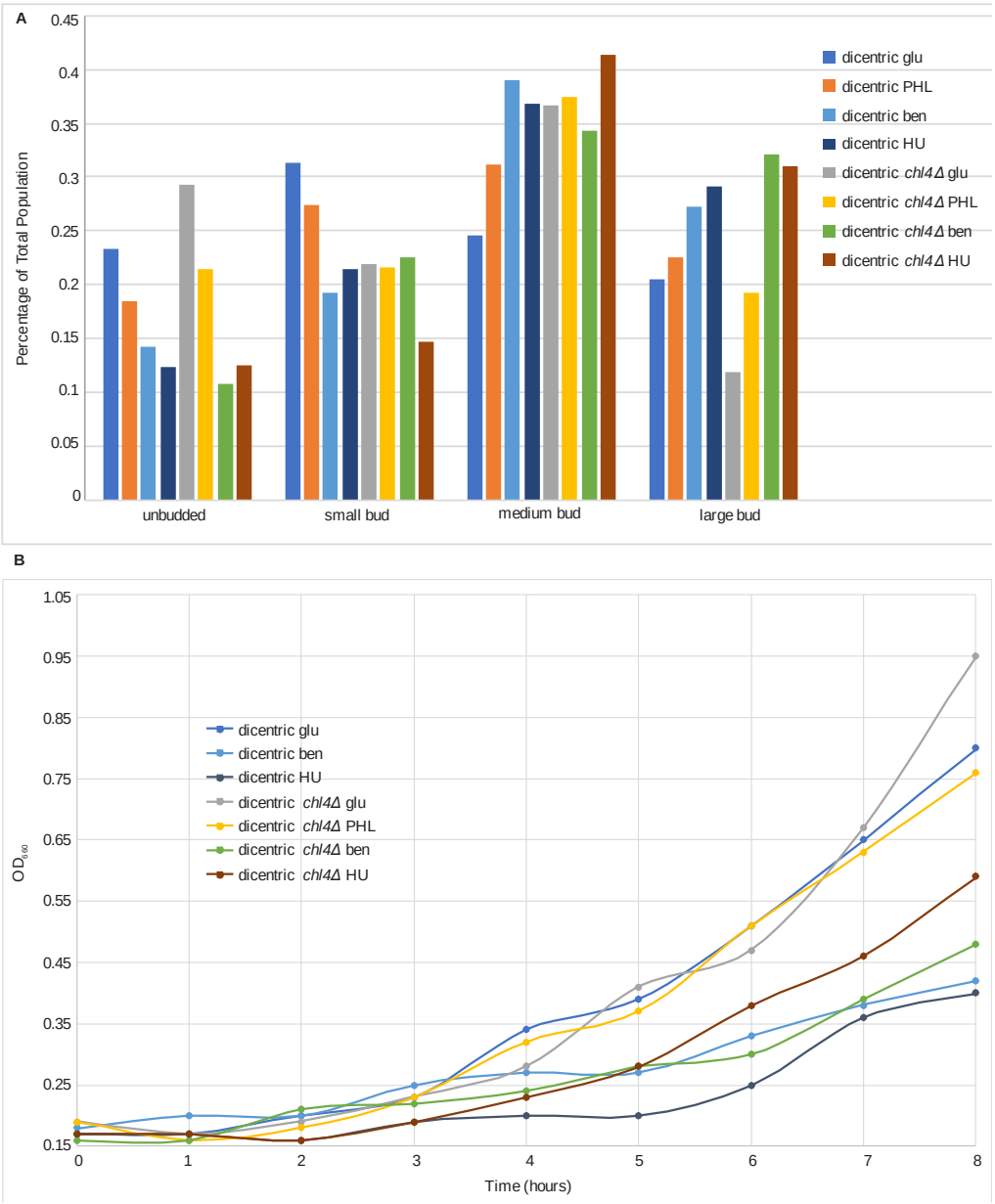

Fig. S2 Cell cycle distributions and growth rates of WT dicentric and dicentric *chl4Δ*
(A) Cells were categorized according to bud size. Cells were treated with 0.2 µg/ml PHL, 5 mM HU, or 0.5 µg/ml benomyl where indicated. Each strain/treatment's distribution is significantly different from the others by Chi squared analysis. No systematic cell cycle delay that corresponds to the ability of the treatment to activate de novo kinetochore assembly was found. Dicentric glu n=557; dicentric PHL n=512; dicentric ben n=519; dicentric HU n=562; dicentric *chl4Δ* glu n=560; dicentric *chl4Δ* PHL n=424; dicentric *chl4Δ* ben n=553; dicentric *chl4Δ* HU n=499. Chi squared p values can be found in Table S3.
(B) Growth rates of WT dicentric and dicentric *chl4Δ* were determined on YPD alone and YPD +0.2 µg/ml PHL, +5 mM HU, and +0.5 µg/ml benomyl. Differences in growth rate do not correlate with de novo kinetochore formation. Each strain was grown over 8 hours and measured every hour.

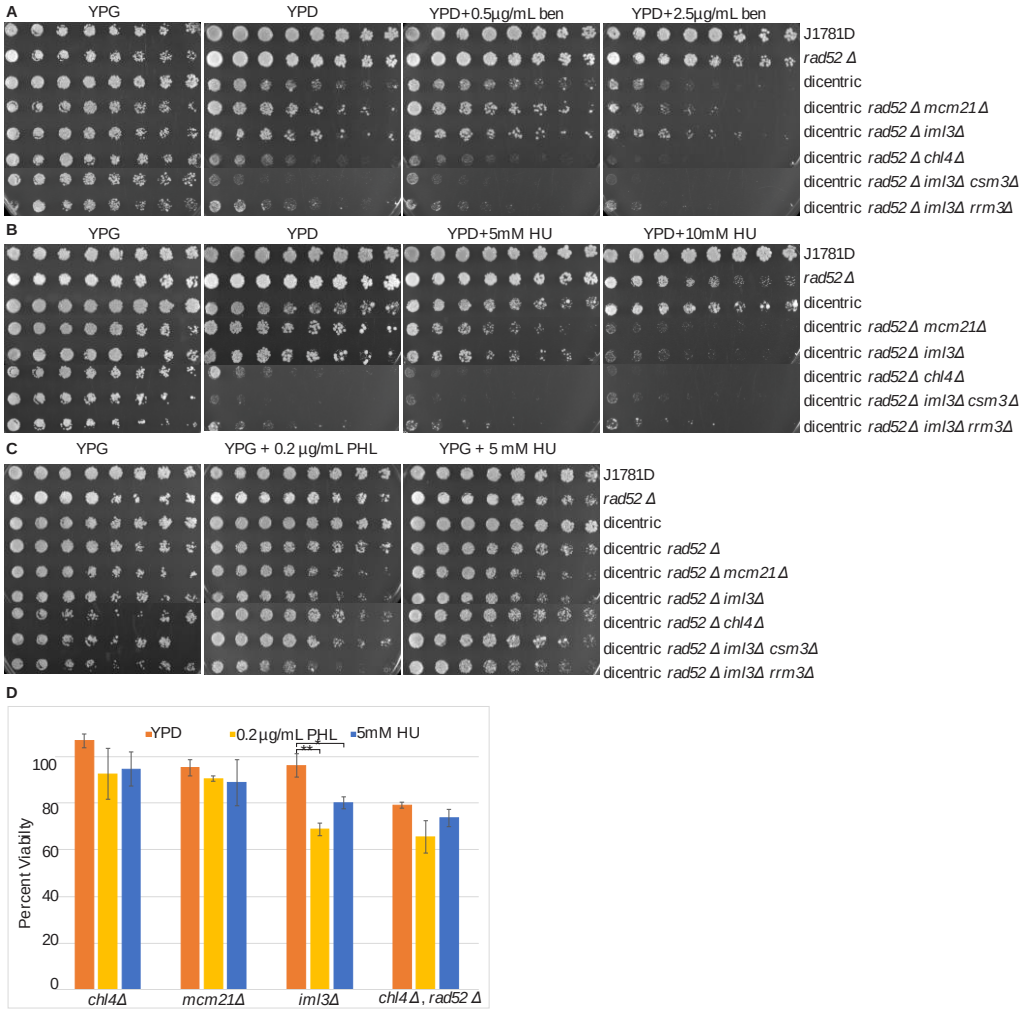

Fig. S3 Serial dilutions in Benomyl, HU and Galactose + PHL or HU

(A) Serial dilutions of WT and various mutants were pronged on galactose (YPG), glucose (YPD), glucose + 0. 5 µg/ml benomyl, and glucose + 2.5 µg/ml benomyl. Dilutions are 2-fold from left to right. Benomyl does not activate the GALCEN in COMA mutants. Prong plates were repeated in triplicate with identical results.

(B)Serial dilutions of WT and various mutants were pronged on galactose (YPG), glucose (YPD), glucose + 5 mM HU, and glucose + 10 mM HU. Dilutions are 2-fold from left to right. A higher concentration of HU has a stronger GALCEN activation effect in COMA mutants. Prong plates were repeated in triplicate with identical results.

(C) Serial dilutions of WT and various mutants were pronged on galactose (YPG), galactose + 0.2 µg/ml phleomycin (PHL), and galactose + 5 mM hydroxyurea (HU). Dilutions are 2-fold from left to right. On galactose (inactive GALCEN), PHL and HU have no effect on dicentric strains. Prong plates were repeated in triplicate with identical results.

(D) Quantitative analysis of cell viability in monocentric single mutants (*chl4Δ*, *iml3Δ*, and *mcm21Δ*) and monocentric double mutant (*chl4Δ*, *rad52Δ)* expressed as a percent of single colony growth on galactose. Error bars are standard error of the mean. Student's T-test p-value for *iml3Δ* YPD vs. PHL is 0.009, for YPD vs. HU, 0.048. Student's T-test p-values can be found in Table S1. Dilution plating ns can be found in Table S2.

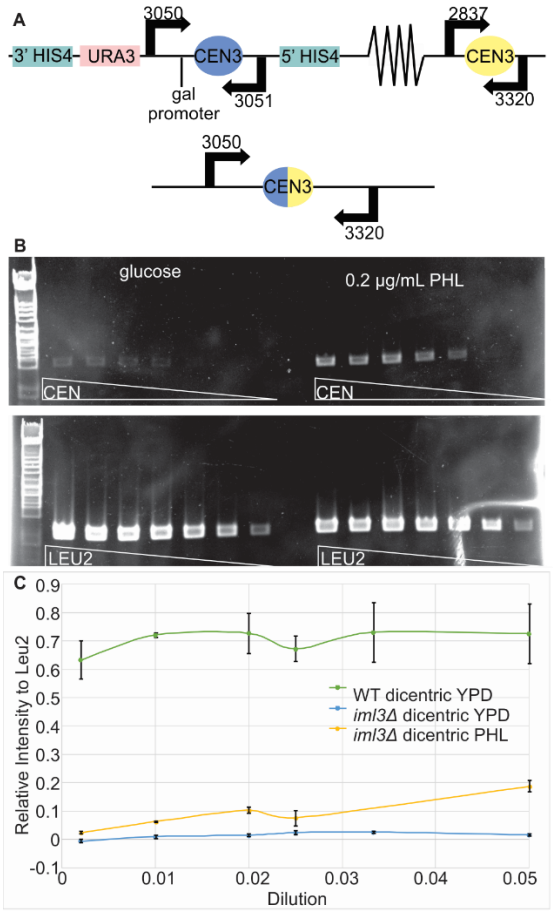

Fig. S4 Physical analysis of dicentric chromosome breakage and rearrangement via homologous recombination

(A) Schematic of dicentric chromosome showing locations of GALCEN3 at the HIS4 gene, and relevant primers used in PCR assays. (B) DNA was isolated from single colonies of dicentric *iml3Δ* mutants grown on YPD and YPD + PHL (0.2 µg/ml), serially diluted, and used as template to probe for homologous recombination between the two centromeres (CEN) (oligonucleotides 3050 and 3320, fragment size 1.1 kb) and LEU2 (control). These cells are proficient for homologous recombination. (C) Quantitation of rearrangement PCR assay with wild-type dicentric control. Integrated intensity of PCR bands was calculated as described in Hoffman et al., (4). Centromere rearrangement (CEN) was normalized to LEU2 band intensity and plotted as a function of DNA template dilution factor. WT dicentric shows elevated levels of rearrangement on YPD, ~70% (5). Rearrangement is evident in dicentric *iml3Δ* on PHL (20%), but not in the absence of PHL (dicentric, *iml3Δ*). Standard marker sizes are identical throughout. Error bars are standard error of the mean. n=2 for each dilution series.

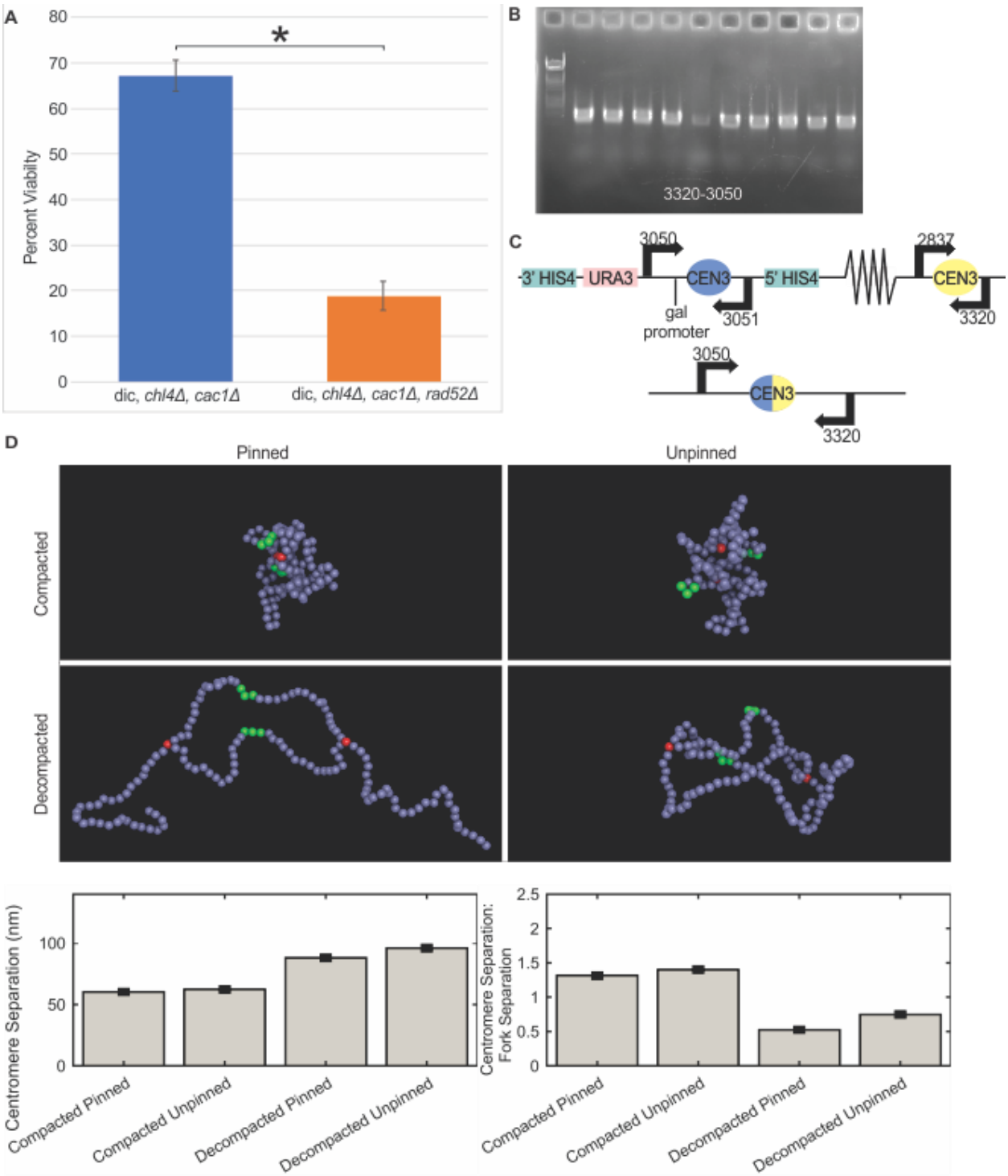

Fig. S5 Role of the chromatin assembly factor, Cac1 in experimental de novo kinetochore assembly and centromere separation in Brownian simulations of a polymer chain

(A) Quantitative analysis of cell viability expressed as a percent of single colony growth on galactose (inactive GALCEN). Deletion of Cac1 suppresses the defect in de novo kinetochore assembly in dicentric, *chl4Δ*. Error bars are standard error of the mean. Student's t-test p-value 0.000483. Dilution plating ns can be found in Table S2.

(B) DNA was isolated from single colonies of dicentric, *chl4Δ, cac1Δ* cells grown on YPD, and used as a template to probe for homologous recombination between the two centromeres (oligonucleotides 3050 and 3320, fragment size 1.1 kb). PCR products were subjected to gel electrophoresis. 10/10 colonies contained the homologous recombination product. Standard marker sizes are identical throughout.
(C) Schematic of dicentric chromosome showing locations of GALCEN3 at the HIS4 gene, and relevant primers used in PCR assays.
(D) Thermodynamic simulation of a pinned and unpinned replication bubble in a 1 micron chain
The DNA (purple beads) is depicted as a chain of 10 nm beads. The chain is 1 μm in length, with a region of replication depicted as a bubble (two chains, 350 nm each, arrows marking the junction between replicated and unreplicated chains) within the 1 micron chain. The origin of replication is the midpoint of the bubble, indicated as green beads. The number of green beads represent the size of the centromere DNA in a 1 micron chain (100 bp, or ~33 nm). The chains are moving in time in two situations, end beads 100X the mass of the remaining beads (pinned) and end beads 1X the mass of the remaining beads (unpinned). Selected frames are shown from timelapse movies. The program was run for 18.2 ms for a total of 15,000 time steps. A frame is extracted every 3.5 μs, thus frame 100 is equivalent to .35 ms. To simulate chromatin compaction (compacted), every seventh bead was linked by a spring with the same spring constant that links consecutive beads. In the decompacted simulations, the intrastrand compaction was removed. The final frames from each simulation are shown. Below the images are bar charts of centromere separation in nm (left) and the ratio of centromere separation to fork separation (right). The data from each run were pooled. Error bars are standard error of the mean. All values are significantly different from each other by a Tukey Test using the Tukey-Kramer method (all P-values < 0.05). Compact pinned n=15,622; compact unpinned n=15,633; decompacted pinned n=15,603; decompacted unpinned n=15,603.

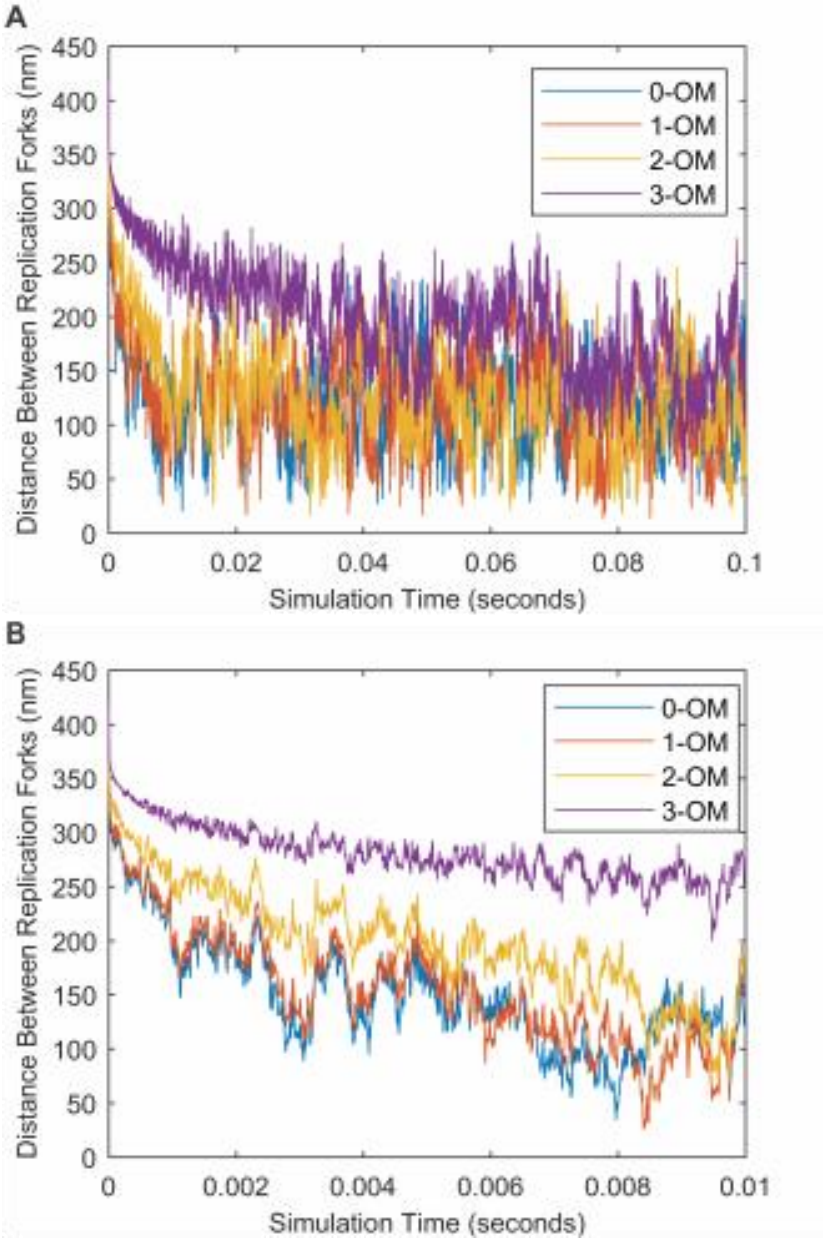

Fig. S6 Estimating the drag force of the chromosome arms

The fork separation of the replication bubble (fork-to-fork distance) was calculated for each time step in the chromoShake model of the replication bubble. These distances were plotted over time for four different iterations the model, which differed in the drag force applied to the end beads (outermost beads from the origin of replication). The drag force applied to the end beads in each of the four simulations were the 1x, 10x, 100x, and 1000x (0-OM, 1-OM, 2-OM, and 3-OM, respectfully) that of the drag force applied to a standard bead. The fork separation over time is plotted over (A) 0.1 seconds of simulation time and (B) 0.01 seconds of simulation time.

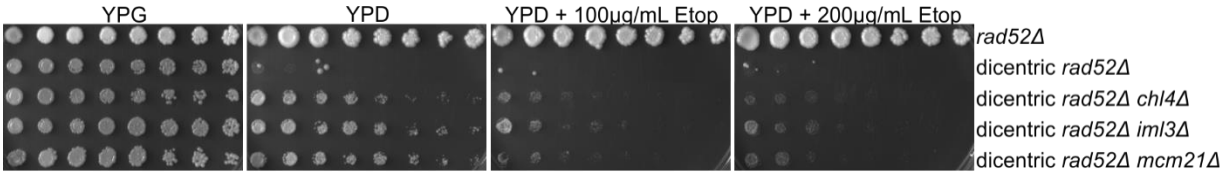

Fig. S7 Rescue of de novo kinetochore assembly in COMA mutants through etoposide treatment
Serial dilutions of *rad52Δ* and various COMA mutants with the dicentric chromosome were pronged on galactose (YPG), glucose (YPD), glucose + 100 µg/ml etoposide, and glucose + 200 µg/ml etoposide plates. Dilutions are 2-fold from left to right. The topoisomerase 2 inhibitor etoposide rescues the kinetochore assembly defect in *chl4Δ*, *iml3Δ*, and *mcm21Δ* mutants containing a conditional GALCEN3 centromere. This is the same pattern of rescue afforded by PHL and HU (Fig. 1). Prong plates were repeated in triplicate with identical results.

Supplemental Tables

Table S1

Student's T-test p-values of Percent Viability

	J1781D YPD	J1781D PHL	J1781D HU
J1781D YPD		0.182676	0.1808183
J1781D PHL	0.182676		0.8115228
J1781D HU	0.1808183	0.8115228	

	rad52Δ YPD	rad52Δ PHL	rad52Δ HU
rad52Δ YPD		0.0562	0.22391
rad52Δ PHL	0.0562		0.10228
rad52Δ HU	0.22391	0.10228	

	dicentric YPD	dicentric PHL	dicentric HU
dicentric YPD		0.0002326	0.061709
dicentric PHL	0.0002326		0.000416
dicentric HU	0.061709	0.0004156	

	dic, rad52Δ YPD	dic, rad52Δ PHL	dic, rad52Δ HU
dic, rad52Δ YPD		0.050769163	0.201433118
dic, rad52Δ PHL	0.05076916		0.024296953
dic, rad52Δ HU	0.20143312	0.024296953	

	dic, rad52Δ, mcm21Δ YPD	dic, rad52Δ, mcm21Δ PHL	dic, rad52Δ, mcm21Δ HU
dic, rad52Δ, mcm21Δ YPD		3.68311E-06	0.001748755
dic, rad52Δ, mcm21Δ PHL	3.68311E-06		0.066270682
dic, rad52Δ, mcm21Δ HU	0.001748755	0.066270682	

	dic, rad52Δ, iml3Δ YPD	dic, rad52Δ, iml3Δ PHL	dic, rad52Δ, iml3Δ HU
dic, rad52Δ, iml3Δ YPD		1.3353E-07	0.007027707
dic, rad52Δ, iml3Δ PHL	1.3353E-07		0.042885351
dic, rad52Δ, iml3Δ HU	0.007027707	0.042885351	

	dic, rad52Δ, chl4Δ YPD	dic, rad52Δ, chl4Δ PHL	dic, rad52Δ, chl4Δ HU
dic, rad52Δ, chl4Δ YPD		0.000153466	0.028275069

dic, rad52Δ, chl4Δ PHL	0.000153466		0.031293372
dic, rad52Δ, chl4Δ HU	0.028275069	0.031293372	

	dic, rad52Δ, scc4m7 YPD	dic, rad52Δ, scc4m7 PHL	dic, rad52Δ, scc4m7 HU
dic, rad52Δ, scc4m7 YPD		0.161488964	0.103841947
dic, rad52Δ, scc4m7 PHL	0.161488964		0.592879037
dic, rad52Δ, scc4m7 HU	0.103841947	0.592879037	

	dic, rad52Δ, iml3Δ, csm3Δ YPD	dic, rad52Δ, iml3Δ, csm3Δ PHL	dic, rad52Δ, iml3Δ, csm3Δ HU
dic, rad52Δ, iml3Δ, csm3Δ YPD		0.195526415	0.164023922
dic, rad52Δ, iml3Δ, csm3Δ PHL	0.195526415		0.294004079
dic, rad52Δ, iml3Δ, csm3Δ HU	0.164023922	0.294004079	

	dic, rad52Δ, ilm3Δ, rrm3Δ YPD	dic, rad52Δ, ilm3Δ, rrm3Δ PHL	dic, rad52Δ, ilm3Δ, rrm3Δ HU
dic, rad52Δ, ilm3Δ, rrm3Δ YPD		0.010618873	0.13103648
dic, rad52Δ, ilm3Δ, rrm3Δ PHL	0.010618873		0.04585707
dic, rad52Δ, ilm3Δ, rrm3Δ HU	0.13103648	0.04585707	

	chl4Δ YPD	chl4Δ PHL	chl4Δ HU
chl4Δ YPD		0.277038837	0.2015217
chl4Δ PHL	0.277038837		0.881524135
chl4Δ HU	0.2015217	0.881524135	

	mcm21Δ YPD	mcm21Δ PHL	mcm21Δ HU
mcm21Δ YPD		0.285516433	0.580040189
mcm21Δ PHL	0.285516433		0.875260791
mcm21Δ HU	0.580040189	0.875260791	

	iml3Δ YPD	iml3Δ PHL	iml3Δ HU
iml3Δ YPD		0.009018536	0.048664136
iml3Δ PHL	0.009018536		0.066028614
iml3Δ HU	0.048664136	0.066284297	

	chl4Δ rad52Δ YPD	chl4Δ rad52Δ PHL	chl4Δ rad52Δ HU
chl4Δ, rad52Δ YPD		0.124524302	0.23182077
chl4Δ, rad52Δ PHL	0.124524302		0.359771962
chl4Δ, rad52Δ HU	0.23182077	0.359771962	

Table S2

Strain	# of platings	# of colonies glu	gal	PHL	HU
J1781D	4	1586	1733	1681	1743
rad52Δ	2	191	218	91	139
dicentric	3(glu, gal, PHL) 2 (HU)	113	156	46	95
dic, rad52Δ	3	366	1466	188	422
dic, rad52Δ, chl4Δ	5(glu, gal, PHL) 2(HU)	876	1338	165	267
dic, rad52Δ, mcm21Δ	5(glu, gal, HU) 4(PHL)	1179	1611	144	465
dic, rad52Δ, iml3Δ	5	1492	2216	88	464
dic, rad52Δ, scc4m7	2	31	573	13	17

dic, rad52Δ, iml3Δ, csm3Δ	6 (glu, gal) 2(PHL, HU)	380	1079	8	6
dic, rad52Δ, ilm3Δ, rrm3Δ	4(glu, gal, HU) 2(PHL)	239	595	36	185
dic, rad52Δ, ctf19Δ	7	1137	2499	n/a	n/a
chl4Δ	3	1637	1537	1397	1445
mcm21Δ	3	3357	3536	3196	3117
iml3Δ	3	1409	1466	1007	1175
chl4Δ, rad52Δ	3	556	703	406	518
Dic, chl4Δ, cac1Δ	3	427	637	n/a	n/a
Dic, chl4Δ, cac1Δ, rad52Δ	3	125	672	n/a	n/a

Table S3

	Dicentric glu	Dicentric PHL	Dicentric ben	Dicentric HU	Dic chl4Δ glu	Dic chl4Δ PHL	Dic chl4Δ ben	Dic chl4Δ HU
Dicentric glu		0.0005089	3.217E-21	1.511E-21	5.860E-17			
Dicentric PHL	0.0005089							
Dicentric ben	3.217E-21							
Dicentric HU	1.511E-21							
Dic chl4Δ glu	5.860E-17					3.278E-06	8.031E-55	4.034E-46
Dic chl4Δ PHL					3.278E-06			
Dic chl4Δ ben					8.031E-55			
Dic chl4Δ HU					4.034E-46			

Table S4

Strains	Genotype
J1781D	MATa ade1 met14 ura3-52 leu2-3,112 his3-11,15
MBY1005	J1781D rad52::LEU2
DCY1044.1	J1781D GALCEN3-URA3::his4
MBY1010	J1781D GALCEN3-URA3::his4 rad52::LEU2
DCY1057.1	J1781D GALCEN3-URA3::his4 chl4::KAN
DCY1079.1	J1781D GALCEN3-URA3::his4 chl4::KAN rad52::LEU2
DCY1074.1	J1781D iml3::KAN GALCEN3-URA3::his4 csm3::NAT rad52::LEU2
DCY1075.1	J1781D iml3::KAN GALCEN3-URA3::his4 rrm3::NAT rad52::LEU2
MBY1012	J1781D mcm21::KAN GALCEN3-URA3::his4 rad52::LEU2
MBY1013	J1781D iml3::KAN GALCEN3-URA3::his4 rad52::LEU2
DCY1082.1	J1781D GALCEN3-URA3::his4 scc4^{m7}:HIS rad52::LEU2
DCY1052.1	J1781D iml3::KAN GALCEN3-URA3::his4
DCY1060.1	J1781D chl4::KAN
DCY1134.1	J1781D chl4::KAN rad52::LEU2
KBY4060	J1781D mcm21::KAN
KBY4061	J1781D iml3::KAN
DCY1078.1	J1781D GALCEN3-URA3::his4 ctf19::NAT rad52::LEU2
DCY1161.1	J1781D GALCEN3-URA3::his4 chl4::KAN cac1::HIS3
DCY1166.1	J1781D GALCEN3-URA3::his4 chl4::KAN cac1::HIS3 rad52::LEU2

References

1. Huang CH, Mirabelli CK, Jan Y, & Crooke ST (1981) Single-strand and double-strand deoxyribonucleic acid breaks produced by several bleomycin analogues. *Biochemistry* 20(2):233-238.
2. Warner HR, Snustad P, Jorgensen SE, & Koerner JF (1970) Isolation of bacteriophage T4 mutants defective in the ability to degrade host deoxyribonucleic acid. *J Virol* 5(6):700-708.
3. Lawrimore J*, et al.* (2016) ChromoShake: a chromosome dynamics simulator reveals that chromatin loops stiffen centromeric chromatin. *Mol Biol Cell* 27(1):153-166.
4. Hoffman DB, Pearson CG, Yen TJ, Howell BJ, & Salmon ED (2001) Microtubule-dependent changes in assembly of microtubule motor proteins and mitotic spindle checkpoint proteins at PtK1 kinetochores. *Mol Biol Cell* 12(7):1995-2009.
5. Mythreye K & Bloom KS (2003) Differential kinetochore protein requirements for establishment versus propagation of centromere activity in *Saccharomyces cerevisiae*. *J Cell Biol* 160(6):833-843.